Available online at www.sciencedirect.com
SCIENCE DIRECT®
International Journal of Heat and Mass Transfer 47 (2004) 3909–3925
International Journal of HEAT and MASS TRANSFER
www.elsevier.com/locate/ijhmt

Resolution of linear inverse forced convection problems using model reduction by the Modal Identification Method: application to turbulent flow in parallel-plate duct

Manuel Girault *, Daniel Petit *

Laboratoire d'Etudes Thermiques, U.M.R. C.N.R.S. n° 6608, Université de Poitiers, ENSMA, Téléport 2, 1 avenue Clément Ader, B.P. 40109, 86961 Futuroscope Cedex, France

Received 3 September 2003; received in revised form 10 February 2004

Abstract

Inverse Heat Convection Problems have received attention only recently. They usually involve the use of a high order model corresponding to the spatial discretization of the domain. In this numerical study, the possibility to quickly solve such a problem with a low order model is analysed. The proposed method can be applied to any forced convection problem, whatever the geometry, as far as it is linear. Starting from a Detailed Model (DM) of the system, the Modal Identification Method is applied to build a Reduced Model (RM), which can be used to solve the inverse problem. The inversion procedure is sequential and requires no iterations. The function specification method is used to stabilize the inverse problem. An illustrative application is given. Turbulent forced convection is considered, with a hydrodynamically fully developed, thermally developing, incompressible, turbulent flow of a newtonian and constant property fluid inside a parallel-plate duct. Axial conduction in the flow is neglected. Two wall heat flux densities, varying with time, are estimated from the knowledge of simulated transient temperature measurements inside the fluid. When solving the inverse problem with RM instead of DM, a drastic reduction of computing time is obtained (with a reduction factor up to 11,000 in the present study), without significant loss of accuracy. Effects of functional form of the unknowns, sensors number and position, measurement error, on the accuracy of estimates are examined.

Keywords: Forced convection; Modal identification; Reduced Model; Inverse method; Estimation of boundary conditions; Sequential algorithm; Future Time Steps

1. Introduction

Many available studies related to heat convection are concerned with the direct problem, that is: having a mathematical model and knowing boundary conditions, one searches to compute the temperature field over the whole domain. Applications in which thermophysical properties, geometric characteristics or boundary conditions are unknown, but temperature measurements are locally available, belong to inverse problems: from the knowledge of experimental data, one searches to estimate the unknowns, boundary conditions for instance.

While inverse heat conduction problems have been studied for several decades, inverse heat convection problems have received attention only recently. The first published works seem to appear at the end of the 1980s. Moreover, whereas numerous direct convection problems, dealing with forced convection as well as mixed or natural convection, have led to extensive theoretical, experimental and numerical researches, investigations in the field of inverse convection remain quite rare. They principally consist in numerical studies, connected with

* Corresponding authors. Tel.: +33-5-4949-8113; fax: +33-5-4949-8101.
E-mail addresses: girault@let.ensma.fr (M. Girault), petit@let.ensma.fr (D. Petit).

0017-9310/$ - see front matter © 2004 Elsevier Ltd. All rights reserved.
doi:10.1016/j.ijheatmasstransfer.2004.04.001

Nomenclature

$A(N,N)$ state matrix for DM
$B(N,p)$ input matrix for DM
b channel half-height, m
b_D, $b_R(q)$ vectors containing the past of the system for DM and RM respectively
$C(q,N)$ output matrix for DM
$C_a(N,N)$ matrix of thermal capacitances
C_D, $C_R(q,p)$ matrices of dynamic sensitivities for DM and RM respectively
C_p specific heat, $J\,kg^{-1}\,K^{-1}$
c^* solid-to-fluid thermal capacitance ratio
D_h hydraulic diameter, m
e wall thickness, m
$F(n,n)$ diagonal state matrix for RM
$G(n,p)$ input matrix for RM
$H(q,n)$ output matrix for RM
$K(N,N)$ matrix of thermal conductances
k time index
L channel length, m
ℓ dimensionless channel length
n RM order
N DM order
nf number of Future Time Steps
nt number of time steps
N_ξ number of nodes in the axial direction
N_η number of nodes in the transverse direction
p dimension of input vector W
Pe Péclet number
Pr Prandtl number
Pr_{turb} turbulent Prandtl number
q dimension of output vector Y
Re Reynolds number based on mean velocity
$S(q,p)$ static matrix (RM)
T temperature, K
t time, s
U velocity, $m\,s^{-1}$
U_m fluid bulk mean velocity, $m\,s^{-1}$
u dimensionless velocity $= U/U_m$
$W(\tau)$, $\dot{W}(\tau)(p)$ input vector function, its derivative with respect to time
$X(\tau)$, $\dot{X}(\tau)(n)$ state vector function for RM, its derivative with respect to time
x axial coordinate, m
$Y(\tau)(q)$ output vector function
y transverse coordinate, m

Abbreviations
DM Detailed Model
FTS Future Time Steps
MIM Modal Identification Method
RM Reduced Model

Greek symbols
α fluid thermal diffusivity, $m^2\,s^{-1}$
α_{eff} effective diffusivity for heat, $m^2\,s^{-1}$
α_{turb} turbulent diffusivity for heat, $m^2\,s^{-1}$
ΔT measurement error, K
ΔT_{ref} characteristic temperature difference, K
Δt time step, s
$\Delta\tau$ dimensionless time step
ε_{eff} dimensionless effective diffusivity for heat
Φ_n, Φ_s dimensionless applied heat flux densities on north and south walls
η dimensionless transverse coordinate $= y/b$
φ_n, φ_s applied heat flux densities on north and south walls, $W\,m^{-2}$
λ thermal conductivity, $W\,m^{-1}\,K^{-1}$
ν fluid kinematic viscosity, $m^2\,s^{-1}$
ν_{turb} turbulent viscosity, $m^2\,s^{-1}$
θ dimensionless temperature
$\theta(\tau)$, $\dot{\theta}(\tau)(N)$ vector function of temperatures, its derivative with respect to time
$\Psi(N)$ vector containing thermal inputs
ρ density, $kg\,m^{-3}$
σ^* standard deviation of added noise, K
σ dimensionless standard deviation of added noise
τ dimensionless time
ξ dimensionless axial coordinate

Superscripts
$\hat{}$ estimated value
$\bullet$ derivation with respect to time
T transposition sign

Subscripts
f relative to fluid
in inlet
s relative to solid

internal flows and the estimation of thermal boundary conditions from temperature measurements, in the flow or at a wall.

One of the first complete studies is concerned with a steady free convection flow in a 2D parallel-plate duct [1]. Temperature and heat flux density spatial distributions at a wall are estimated from measurements at the opposite wall, using the function specification method [2].

A few inverse problems of natural convection (in cavity) have been explored. These problems, nonlinear in essence, require iterative methods to perform the

inversion. The conjugate gradient method coupled with the resolution of direct, sensitivity and adjoint problems [3,4], is mostly employed. It was used for the estimation of space and time varying wall heat flux density [5] from measurements at the opposite wall. The identification of wall heat flux density spatial distribution from temperature measurements in the fluid, has been performed, either with immovable sensors [6] and mobile ones [7]. In order to reduce the size of direct, sensitivity and adjoint problems to be solved at each iteration of the inverse procedure, the Karhunen–Loève–Galerkin method [8] has been used to build a low dimensional natural convection model for the estimation of a time varying heat source intensity [9]. Conjugate gradient method has also been used to estimate wall heat flux density from temperature measurements in the fluid, for different values of Rayleigh number [10]. A sequential approach based on Kalman filter has also been employed to identify a time varying heat source intensity, in conjunction with the Karhunen–Loève–Galerkin method [11].

Inverse forced convection problems have received more attention, certainly because of their greater simplicity. The flow regime, laminar or turbulent, as well as the flow geometry, do not have a priori any influence on the inverse methodology to use. Conversely, the linearity of the problem with respect to temperature is of importance. If fluid properties vary with temperature, the problem is nonlinear and iterative methods are required. If only the fluid thermal conductivity and specific heat are temperature-dependent, the velocity field may be calculated prior to the inverse problem concerned with the nonlinear energy equation. If the fluid viscosity or density changes with temperature, coupled mass conservation, Navier–Stokes and energy equations have to be considered. In the case of fluid properties supposed independent of temperature, the velocity field may be calculated and only the linear energy equation is considered in the inverse problem. Noniterative inversion methods may then be employed.

In that last linear case, the most used method is however iterative. It employs the conjugate gradient method coupled with the resolution of direct, sensitivity and adjoint problems [3,4].

Flows in parallel-plate ducts, with steady or unsteady heat transfer, have been particularly studied, especially in laminar regime. Following estimations may be reported, using the previous methodology:

- spatial wall heat flux density [12],
- timewise inlet temperature from downstream measurements [13],
- inlet temperature profile in steady regime [14],
- space and time varying wall heat flux density [15],
- time varying wall heat flux density for nonnewtonian fluid flow [16].

The estimation of time varying wall heat flux density for a turbulent flow in parallel-plate duct from temperature measurements in the fluid has also been performed using the same method [17].

Simultaneous estimation of two space and time varying wall heat flux densities in 2D irregularly shaped channels has been performed employing the same methodology [18].

A 3D problem concerning a flow in an irregular shaped duct has been studied using the conjugate gradient method [19]. The aim was to identify a timewise wall heat flux density.

The Levenberg–Marquardt method has been used for the estimation of spatial wall heat flux density for a turbulent flow in a circular duct, in steady regime [20].

The simplex method has been employed to identify spatial wall heat flux density for a laminar flow in parallel-plate duct, after reduction of the model size through a singular perturbations method [21].

Surprisingly, noniterative methods have rarely been used for linear problems. The explanation may be found in the great generality of iterative methods. One can notice that noniterative inversion of a state space representation model has been employed to simultaneously estimate inlet temperature and wall heat flux density for a steady laminar flow in a circular duct [22].

Works connected with nonlinear Inverse forced convection problems are quite uncommon. The estimation of inlet temperature profile in steady laminar polymer melt flow through a narrow channel [23] where fluid properties strongly depend on temperature, has been performed using successive approximations method combined with Tikhonov's regularization [24]. The case of a fluid whose thermal conductivity depends on temperature, flowing in a parallel-plate duct, has also been considered [25]. Authors employ the Karhunen–Loève–Galerkin method to build a Reduced Model used through the conjugate gradient method to estimate a spacewise wall heat flux density in steady regime.

In the present paper, a method for solving linear transient inverse forced convection problems is proposed. The inverse algorithm is noniterative, sequential, and includes the function specification method [2]. The main originality is the use of Reduced Models (RM) to perform the inversion. The Modal Identification Method (MIM) [26,27] is used to build RMs. An illustrative example is given, involving a turbulent flow in a parallel-plate duct. Turbulent forced convection inside ducts is of common use in heat exchangers. Such thermal equipment is frequently subject to variation of wall heat fluxes with time, that may induce undesirable thermal stresses. Heat exchangers control is therefore an important problem. In the proposed example, two time varying wall heat flux densities, respectively applied on the upper and lower plates of the duct, are simultaneously estimated from the knowledge of temperature readings

taken at specific locations inside the fluid. Estimations obtained using RMs are compared to those obtained using a classical Detailed Model (DM) of the system built with the Finite Volume Method.

The following points will be developed:

- In Section 2, heat transfer modelling using state space representation is introduced.
- In Section 3, solutions of direct and inverse problems using DM are given.
- In Section 4, the Modal Identification Method (MIM) used to build a RM of DM, is briefly presented.
- In Section 5, solutions of direct and inverse problems using RM are developed.
- In Section 6, Future Time Steps [2] are introduced in order to stabilize solutions.
- In Section 7, the system used as example is described, governing heat transfer equation and associated boundary conditions are written.
- In Section 8, studied configuration, sensitivity analysis, inversion results and comparison between estimations obtained using RM and DM, are presented.
- In Section 9, some conclusions and prospects are proposed.

2. Heat transfer modelling using state space representation

Let us consider a linear thermal system. Whatever the dimension of the problem, its geometry and the spatial discretization method (finite differences, finite volumes, finite elements, ...), the energy equation and associated boundary conditions can be written in the matrix form:

$$C_a\dot{\theta}(\tau) = K\theta(\tau) + \Psi(\tau) \tag{1}$$

where $\theta(\tau)$ (dim. N) is the vector function of temperatures at the N discretization nodes, $\dot{\theta}(\tau)$ its derivative with respect to time τ, C_a (dim. N,N) is the matrix of thermal capacities, K (dim. N,N) is the matrix of conductances and $\Psi(\tau)$ (dim. N) is the vector function containing thermal inputs (boundary conditions and/or internal heat sources) for each node of discretization.

$$\text{By writing:} \quad \begin{cases} A = C_a^{-1}K \\ BW(\tau) = C_a^{-1}\Psi(\tau) \end{cases} \tag{2}$$

$$\text{Eq. (1) becomes:} \quad \dot{\theta}(\tau) = A\theta(\tau) + BW(\tau) \tag{3}$$

State matrix A (dim. N,N) links temperatures at discretization nodes and input matrix B (dim. N,p) links discretization nodes to thermal inputs gathered in vector W (dim. p).

An output matrix C (dim. q,N) allows to select q temperatures in the whole temperature field and to store them in vector function Y:

$$Y(\tau) = C\theta(\tau) \tag{4}$$

Eqs. (3) and (4) constitute a Detailed Model (DM) of the system, called *state space representation*:

$$\dot{\theta}(\tau) = A\theta(\tau) + BW(\tau) \tag{5a}$$

$$Y(\tau) = C\theta(\tau) \tag{5b}$$

3. Direct and inverse problems using DM

The direct problem consists in calculating θ knowing A and B (the model) as well as W (thermal inputs). Output vector Y can then be extracted.

Time discretization ($\Delta\tau$ being the time step) of Eqs. (5a) and (5b) using a fully implicit scheme leads, at step $(k+1)$, to the linear relation between output vector $Y(k+1)$ and input vector $W(k+1)$:

$$(I - A\Delta\tau)\theta(k+1) = B\Delta\tau W(k+1) + \theta(k) \tag{6a}$$

$$Y(k+1) = C\theta(k+1) \tag{6b}$$

The resolution of the direct problem can be done using methods for solving linear systems, avoiding any inversion of the dimension N matrix $(I - A\Delta\tau)$.

The inverse problem we consider consists in estimating W, knowing A, B and some part Y of θ. Rearranging Eqs. (6a) and (6b), one obtains:

$$C_{\mathrm{D}}W(k+1) = Y(k+1) - b_{\mathrm{D}}(k) \tag{7}$$

$$\text{with} \quad C_{\mathrm{D}} = C(I - A\Delta\tau)^{-1}B\Delta\tau \tag{8}$$

$$\text{and} \quad b_{\mathrm{D}}(k) = C(I - A\Delta\tau)^{-1}\theta(k) \tag{9}$$

With the assumption that we have at least as many sensors as unknowns ($q \geqslant p$), Eq. (7) may be solved for $W(k+1)$ using linear least squares, to get an estimation $\widehat{W}(k+1)$ of $W(k+1)$:

$$\widehat{W}(k+1) = \left(C_{\mathrm{D}}^{\mathrm{T}} \cdot C_{\mathrm{D}}\right)^{-1} C_{\mathrm{D}}^{\mathrm{T}}(Y(k+1) - b_{\mathrm{D}}(k)) \tag{10}$$

Remark. The inversion of a dimension N matrix is needed to compute C_{D} and $b_{\mathrm{D}}(k)$ (cf. Eqs. (8) and (9)), and obtain this solution.

4. Model reduction using the Modal Identification Method

In order to avoid the inversion of a high dimension matrix, we propose to use a low dimensional model, also called Reduced Model (RM), whose behaviour is as close as possible to DM (Eqs. (5a) and (5b)). The linearity of these equations allows us to apply the *Modal Identification Method* [26,27]. It consists in an identification procedure performed in one single step, which is briefly presented hereafter and leads to the modal matrix form:

$$\dot{X}(\tau) = FX(\tau) + G\dot{W}(\tau) \tag{11a}$$

$$Y(\tau) = HX(\tau) + SW(\tau) \tag{11b}$$

X is a new state space vector of low dimension n ($n \ll N$), F is a diagonal matrix containing n dominant "eigenvalues" of the system, $\dot{W}$ is the derivative with respect to time of input vector W. G is the input matrix. Output vector Y is wanted to be very close to the one defined by Eq. (5b). H and S are respectively called output and static matrices. *All the matrices included in Eqs.* (11a) *and* (11b) *come from an identification procedure (not a diagonalization) when decreasing unit steps are applied separately and successively on each of the two components of* W. The procedure consists in minimizing a squared residues functional relative to the difference between an output vector simulated with DM (Eqs. (5a) and (5b)) and the analytical output solution of Eqs. (11a) and (11b).

Such Reduced Models have been used in previous works to solve multidimensional direct and inverse linear heat conduction problems [27–31].

Thanks to its small order, computing time is strongly reduced when using RM.

5. Direct and inverse problems using RM

An analytical solution of Eqs. (11a) and (11b) between time nodes k and $k+1$ leads to the following time discretization [27]:

$$X(k+1) = \exp(F\Delta\tau)[X(k) + G(W(k+1) - W(k))] \tag{12a}$$

$$Y(k+1) = HX(k+1) + SW(k+1) \quad \text{(direct problem)} \tag{12b}$$

Rearranging Eqs. (12a) and (12b), one obtains:

$$C_{\mathrm{R}}W(k+1) = Y(k+1) - b_{\mathrm{R}}(k) \tag{13}$$

$$\text{with} \quad C_{\mathrm{R}} = H\exp(F\Delta\tau)G + S \tag{14}$$

$$\text{and} \quad b_{\mathrm{R}}(k) = H\exp(F\Delta\tau)(X(k) - GW(k)) \tag{15}$$

With the assumption that we have at least as many sensors as unknowns ($q \geqslant p$), Eq. (13) may be solved for $W(k+1)$ using linear least squares:

$$\widehat{W}(k+1) = \left(C_{\mathrm{R}}^{\mathrm{T}} \cdot C_{\mathrm{R}}\right)^{-1} C_{\mathrm{R}}^{\mathrm{T}}(Y(k+1) - b_{\mathrm{R}}(k)) \quad \text{(solution of inverse problem)} \tag{16}$$

Remark. In contrast to Eq. (10), no inversion of a dimension N matrix is needed to obtain Eq. (16). The matrix F being diagonal, C_{R} (Eq. (14)) and $b_{\mathrm{R}}(k)$ (Eq. (15)) are easily computed.

6. Function specification method

Until now, it has been considered that at any time step $(k+1)$, heat fluxes sent through $W(k+1)$ have an immediate influence on sensors, i.e. $Y(k+1)$. That was without taking into account the lagging and damping effects of the heat transfer equation. In the present study they are due essentially to the wall heat storage. As $W(k+1)$ might have no real influence on $Y(k+1)$, and might be "seen" only at time step $(k+2)$ or later, it is very useful to introduce *Future Time Steps (FTS)* [2], that is: using sensors information at time steps $(k+2)$, $(k+3), \ldots$, to correctly estimate $W(k+1)$. By using this extra information, the function specification method also acts as a regularization procedure which stabilizes the solution. If nf is the number of FTS to be used, then for $1 \leqslant f \leqslant \mathrm{nf}$, Eq. (10) or Eq. (16) (depending on the model which is used, DM or RM) is written for $W(k+1+f)$ and $Y(k+1+f)$. A temporary approximation of $W(k+1+f)$ is needed to compute $W(k+1)$. The function specification method [2] is used, so it is assumed that: $W(k+1+f) = W(k+1)$ for $1 \leqslant f \leqslant \mathrm{nf}$.

With a macrovector $Y' = [Y(k+1), Y(k+2), \ldots, Y(k+1+\mathrm{nf})]^{\mathrm{T}}$, the $\mathrm{nf}+1$ equations can be written under a macrovector form either for DM and RM:

$$C'W(k+1) = Y' - b'(k) \tag{17}$$

where matrix C' and vector $b'(k)$ depend on the model used for inversion (DM or RM).

The solution of Eq. (17) using linear least squares is then given by:

$$\widehat{W}(k+1) = \left(C'^{\mathrm{T}} \cdot C'\right)^{-1} C'^{\mathrm{T}}\left(Y' - b'(k)\right) \tag{18}$$

7. An illustrative example: turbulent forced convection in parallel-plate duct

7.1. Description of the physical system and its mathematical model

Turbulent forced convection is considered, with a hydrodynamically fully developed, thermally developing, incompressible, turbulent flow of a newtonian and constant property fluid inside a parallel-plate duct. Channel walls are supposed to be smooth. Axial conduction in the fluid and viscous dissipation are neglected. Conduction along the flow in the wall material is disregarded. The assumption of uniform wall temperature across the whole thickness of the plates is made. A pseudo-laminar model is taken as turbulent model.

Applied thermal boundary conditions are:

- uniform fluid inlet temperature T_{in},
- two heat flux densities $\varphi_{\mathrm{n}}(t)$ and $\varphi_{\mathrm{s}}(t)$ applied on external surface of channel plates, a priori different and varying with time.

Let us call L the channel length, b the half-height, e the wall thickness, v the kinematic viscosity of the fluid, λ its thermal conductivity, α its thermal diffusivity, $(\rho C_p)_f$ and $(\rho C_p)_s$ the volumic heat capacity respectively for fluid and solid, $U(y)$ the fully developed turbulent velocity distribution, $\alpha_{turb}(y)$ the turbulent diffusivity distribution and $T(x,y,t)$ the mean statistic temperature at position (x,y) and time t. A schematic view of the system is presented in Fig. 1.

Under previous hypothesis, the transient energy equation may be written:

$$\frac{\partial T}{\partial t}(x,y,t) + U(y)\frac{\partial T}{\partial x}(x,y,t) = \frac{\partial}{\partial y}\left(\alpha_{eff}(y)\frac{\partial T}{\partial y}(x,y,t)\right) \quad (19)$$

$\forall x \in]0,L[, \forall y \in [-b,+b[, \forall t > 0$, and where the effective diffusivity $\alpha_{eff}(y)$ is the sum of the fluid thermal diffusivity and the turbulent diffusivity $\alpha_{turb}(y)$:

$$\alpha_{eff}(y) = \alpha + \alpha_{turb}(y) \quad (20)$$

Thermal boundary conditions associated with Eq. (19) are written:

- $T(0,y,t) = T_{in}, \quad -b < y < +b, \ t > 0$ (21)
- $\lambda_f \frac{\partial T}{\partial y}(x,+b,t) = \varphi_n(t) - (\rho C_p)_s e \frac{\partial T}{\partial t}(x,+b,t)$ $\forall x \in [0,L], \ \forall t > 0$ (22)
- $-\lambda_f \frac{\partial T}{\partial y}(x,-b,t) = \varphi_s(t) - (\rho C_p)_s e \frac{\partial T}{\partial t}(x,-b,t)$ $\forall x \in [0,L], \ \forall t > 0$ (23)

Boundary conditions defined by Eqs. (22) and (23) take into account both applied heat fluxes and wall heat storage [32,33].

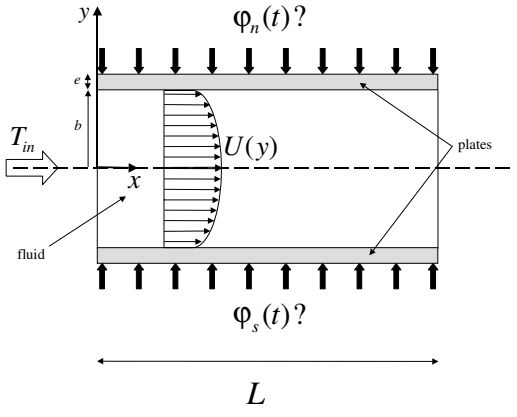

Fig. 1. System description.

The initial condition is written:

$$T(x,y,0) = T_{in} \quad \forall x \in [0,L], \ \forall y \in [-b,+b] \quad (24)$$

Eqs. (19)–(24) may be rewritten in dimensionless form using the following quantities:

$$\xi = \frac{4x}{bPe}, \quad u = \frac{U}{U_m}$$

$$\eta = \frac{y}{b} \quad \text{and} \quad \varepsilon_{eff} = \frac{\alpha_{eff}}{\alpha} = 1 + \frac{\alpha_{turb}}{\alpha}$$

(dimensionless effective diffusivity)

$$\tau = \frac{\alpha t}{b^2}, \quad \theta = \frac{T - T_{in}}{\Delta T_{ref}}$$

$$\text{with} \quad \begin{cases} \Pr = \dfrac{v}{\alpha} \\ Re = \dfrac{U_m D_h}{v} = \dfrac{4bU_m}{v} \\ Pe = RePr = \dfrac{U_m D_h}{\alpha} = \dfrac{4bU_m}{\alpha} \end{cases}$$

where $D_h = 4b$ (hydraulic diameter)

Pr, *Re* and *Pe* are respectively *Prandtl*, *Reynolds and Péclet* numbers and U_m is the fluid bulk mean velocity:

$$U_m = \frac{1}{2b}\int_{y=-b}^{y=b} u(y)\,dy \quad (25)$$

A reference temperature difference is arbitrarily taken as $\Delta T_{ref} = 10$ K (corresponding to the maximal temperature elevation for which the linearity assumption is considered to be valid).

The dimensionless energy equation is written as follows:

$$\frac{\partial \theta}{\partial \tau}(\xi,\eta,\tau) + u(\eta)\frac{\partial \theta}{\partial \xi}(\xi,\eta,\tau) = \frac{\partial}{\partial \eta}\left(\varepsilon_{eff}(\eta)\frac{\partial \theta}{\partial \eta}(\xi,\eta,\tau)\right) \quad \forall 0 < \xi < \ell, \ -1 < \eta < +1, \ \tau > 0 \quad (26)$$

where $\ell = \frac{4L}{bPe}$ is the dimensionless channel length.

$\Phi(\tau) = \frac{\varphi(t)b}{\lambda_f \Delta T_{ref}}$ is a dimensionless heat flux density and $c^* = \frac{(\rho C_p)_s e}{(\rho C_p)_f b}$ is the solid-to-fluid thermal capacitance ratio.

Thermal boundary conditions associated with Eq. (26) are written, from Eqs. (21)–(23):

- $\theta(0,\eta,\tau) = 0, \quad -1 < \eta < +1, \ \tau > 0$ (27)
- $\frac{\partial \theta}{\partial \eta}(\xi,+1,\tau) = \Phi_n(\tau) - c^* \frac{\partial \theta}{\partial \tau}(\xi,+1,\tau)$ $\forall \xi \in [0,\ell], \ \forall \tau > 0$ (28)
- $-\frac{\partial \theta}{\partial \eta}(\xi,-1,\tau) = \Phi_s(\tau) - c^* \frac{\partial \theta}{\partial \tau}(\xi,-1,\tau)$ $\forall \xi \in [0,\ell], \ \forall \tau > 0$ (29)

The initial condition is written from Eq. (24) :

$$\theta(\xi,\eta,0)=0 \quad \forall\xi\in[0,\ell],\ \forall\eta\in[-1,+1] \tag{30}$$

Distributions of dimensionless fully developed turbulent velocity $u(\eta)$ and dimensionless total diffusivity $\varepsilon_{\text{eff}}(\eta)$ in Eq. (26) are determined by the turbulent model given in [34], except for the turbulent Prandtl number: $Pr_{\text{turb}}=\frac{\nu_{\text{turb}}}{\alpha_{\text{turb}}}$ (ν_{turb} being the eddy viscosity), taken as: $Pr_{\text{turb}}=0.85+\frac{0.015}{Pr}$ [35].

7.2. Numerical simulation of temperature measurements

Eq. (26) being linear and parabolic in ξ, it is possible to solve Eqs. (26)–(30) using a sequential procedure in ξ. Let us call N_ξ and N_η the numbers of discretization nodes along the ξ and η directions respectively. N_ξ problems of order N_η are successively solved (at all time steps) instead of a single problem of order $N=N_\xi\times N_\eta$. Using the Finite Volume Method to discretize Eqs. (26)–(29), these problems may be written under *state space representation*:

$$\dot\theta_i(\tau)=A_S\theta_i(\tau)+B_S\begin{bmatrix}\theta_{i-1}(\tau)\\ W(\tau)\end{bmatrix}\quad \forall i\in\langle 1,N_\xi\rangle \tag{31}$$

where θ_i (dim. N_η) is the vector function of dimensionless temperatures at the N_η discretization nodes of the ith channel elementary section, all components of vector θ_0 being equal to the dimensionless inlet temperature according to Eq. (27). $\dot\theta_i(\tau)$ is the derivative with respect to time of $\theta_i(\tau)$ and $W(\tau)=[\,\Phi_n(\tau)\quad\Phi_s(\tau)\,]^T$ (dim. 2) is the heat flux density input vector function containing $\Phi_n(\tau)$ and $\Phi_s(\tau)$. A_S (dim. N_η,N_η) and B_S (dim. N_η,2) are respectively the state and input matrices relative to a channel elementary section whose length is:

$$\Delta\xi=\frac{\ell}{(N_\xi-1)}$$

According to a mesh sensitivity analysis, a nonregular mesh along the η direction (refined near walls) using $N_\eta=25$ for each channel section, and a regular mesh along the ξ direction using $N_\xi=100$ for the whole duct length ($L=200b=50D_h$ i.e. $\xi=800/Pe$), have been chosen. N_ξ is adapted to solve the problem for a portion of the channel length: for instance, to solve up to $x=5D_h$ i.e. $\xi=80/Pe$, $N_\xi=10$.

$\Delta t=10$ s is used as time step. The dimensionless time step is therefore $\Delta\tau=0.09$. 100 time steps are used. The same time step will be employed for the inverse problem.

Functions $\Phi_n(\tau)$ and $\Phi_s(\tau)$ shown in Fig. 2 are used as test functions. The direct problem is solved with these input signals to simulate temperature evolutions. These

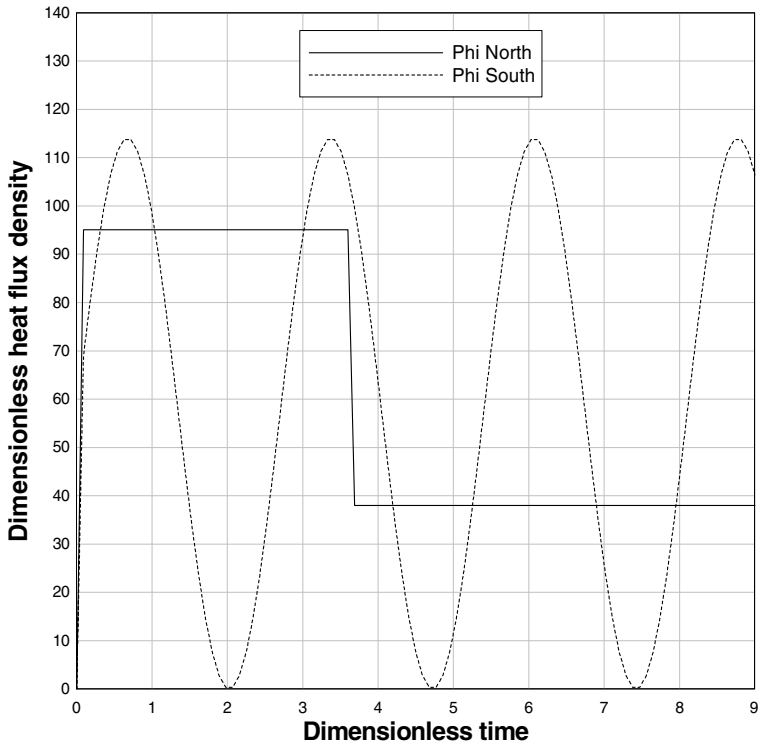

Fig. 2. Test functions $\Phi_n(\tau)$ and $\Phi_s(\tau)$.

Table 1
Sensors names and locations

$\eta = y/b$	$\xi Pe/16 = x/D_h$					
	5	10	20	30	40	50
0.9	P_0	P_1	P_2	P_3	P_4	P_5
0.7	M_0	M_1	M_2	M_3	M_4	M_5
−0.7	M'_0	M'_1	M'_2	M'_3	M'_4	M'_5
−0.9	P'_0	P'_1	P'_2	P'_3	P'_4	P'_5

response signals will be perturbed with an additive numerical random noise to simulate real measurements to be used as data for the inverse problem.

A set of points in the fluid domain is defined in Table 1 and shown in Fig. 3, with their names and locations. They constitute possible sensor locations for the inverse problem.

Figs. 4 and 5 show simulated temperature measurements at P_0, P'_0, P_5, P'_5 and M_0, M'_0, M_5, M'_5 respectively, when random gaussian noise is added to "exact values" obtained by the direct problem resolution. For a discrete temperature evolution T containing the initial temperature and nt time steps, one has:

$$T_i = T_i^{\text{exact}} + \omega_i \frac{\sigma^*}{\Delta T_{\text{ref}}} = T_i^{\text{exact}} + \frac{\Delta T_i}{\Delta T_{\text{ref}}} \quad \forall i \in \langle 0, \text{nt} \rangle$$

where σ^* is the dimensional standard deviation of measurement errors which is assumed to be the same for all measurements and $\{\omega_i\}$ is a gaussian random distribution of mean value 0 and variance 1. That means there is a 99% probability of the value for ω_i to be in the range $-2.576 < \omega_i < +2.576$, hence $\sigma^* = 3.88 \times 10^{-2}$ K corresponds to $-0.1\ \text{K} < \Delta T_i < +0.1\ \text{K}$.

7.3. Inverse problem

The inverse problem we consider consists in estimating $W(\tau) = [\Phi_n(\tau) \quad \Phi_s(\tau)]^T$ from the knowledge of some part of the set of simulated transient temperature measurements previously defined in Section 7.2 (see Table 1 and Fig. 3).

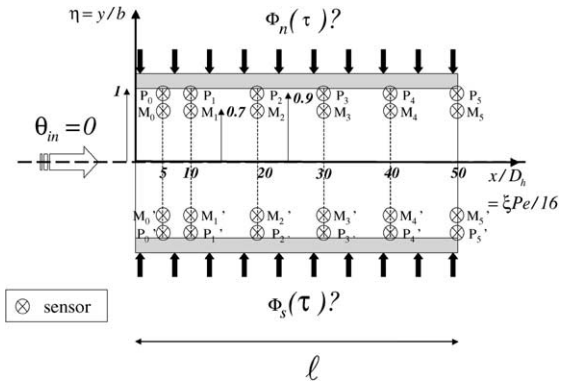

Fig. 3. Sensors location.

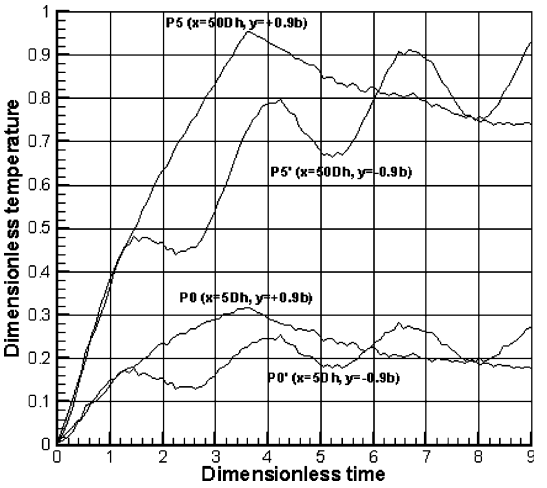

Fig. 4. Simulated temperature measurements at P_0 ($x = 5D_h$, $y = +0.9b$), P'_0 ($x = 5D_h, y = -0.9b$), P_5 ($x = 50D_h, y = +0.9b$), P'_5 ($x = 50D_h, y = -0.9b$).

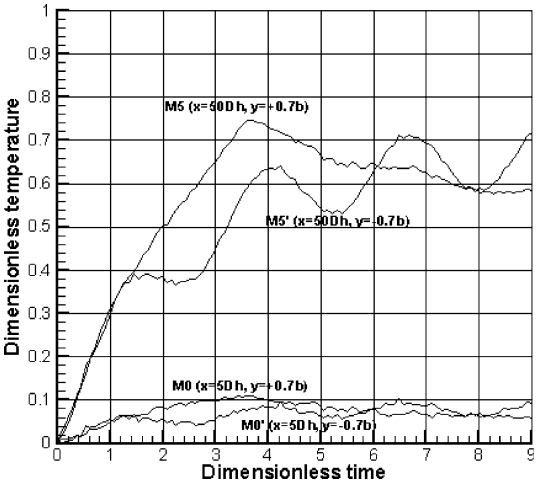

Fig. 5. Simulated temperature measurements at M_0 ($x = 5D_h$, $y = +0.7b$), M'_0 ($x = 5D_h, y = -0.7b$), M_5 ($x = 50D_h, y = +0.7b$), M'_5 ($x = 50D_h, y = -0.7b$).

Table 2
Estimation results for different inversion cases (noise $\sigma = \sigma^*/\Delta T_{\text{ref}} = 3.88 \times 10^{-3}$)

Sensors number and position	Model and value of nf	σ_Y	σ_W	$C'^{\mathrm{T}} \cdot C'$ condition number
2, P_0 and P'_0	DM (order 250) nf = 2	3.915×10^{-3}	7.572	1.0004
2, P_0 and P'_0	RM (order 4) nf = 2	3.918×10^{-3}	7.637	1.0004
2, P_5 and P'_5	DM (order 2500) nf = 2	5.134×10^{-3}	4.458	1.4981
2, P_5 and P'_5	RM (order 8) nf = 2	5.137×10^{-3}	4.604	1.5010
10, P_1 to P_5 and P'_1 to P'_5	DM (order 2500) nf = 1	3.928×10^{-3}	3.369	1.2458
10, P_1 to P_5 and P'_1 to P'_5	RM (order 16) nf = 1	3.932×10^{-3}	3.455	1.2440
2, M_0 and M'_0	DM (order 250) nf = 4	4.200×10^{-3}	11.327	1.0033
2, M_0 and M'_0	RM (order 12) nf = 4	4.200×10^{-3}	11.450	1.0033
2, M_5 and M'_5	DM (order 2500) nf = 2	4.559×10^{-3}	5.252	2.0495
2, M_5 and M'_5	RM (order 17) nf = 2	4.558×10^{-3}	5.362	2.0491
10, M_1 to M_5 and M'_1 to M'_5	DM (order 2500) nf = 2	4.389×10^{-3}	3.984	1.5920
10, M_1 to M_5 and M'_1 to M'_5	RM (order 8) nf = 2	4.393×10^{-3}	4.138	1.5918

It seems not possible to solve the inverse problem for the estimation of $\Phi_{\text{n}}(\tau)$ and $\Phi_{\text{s}}(\tau)$ by using successive equations (31) without employing an iterative procedure. Let us consider temperature data in the ith channel section. The inversion of the corresponding Eq. (31) requires the knowledge of all temperatures in the $i-1$th section. But these temperatures can only be calculated if $\Phi_{\text{n}}(\tau)$ and $\Phi_{\text{s}}(\tau)$ and temperatures in the $i-2$th section are known. One understands that two ways may be chosen to realize the inversion with a Detailed Model.

The first one consists in the use of an iterative method with a sequential procedure in ξ at each iteration: starting with initial guesses $\Phi_{\text{n0}}(\tau)$ and $\Phi_{\text{s0}}(\tau)$, Eqs. (31) are successively solved to compute temperatures at data locations in the ith channel section; the discrepancy between computed and "measured" temperatures can then be minimized using the conjugate gradient method, for example.

The second one, which is used in this paper, is to perform a noniterative procedure, global in ξ. If the Finite Volume Method is used to discretize Eqs. (26)–(29), the problem of order $N = N_\xi \times N_\eta$ may be written under *state space representation* in the form of Eqs. (5a) and (5b):

$$\begin{cases} \dot{\theta}(\tau) = A\theta(\tau) + BW(\tau) \\ Y(\tau) = C\theta(\tau) \end{cases}$$

θ (dim. N) is the vector function of dimensionless temperatures at the N discretization nodes, $\dot{\theta}$ its derivative with respect to dimensionless time τ. A is (N, N) and B is $(N, 2)$. The noniterative approach presented in Section 3 can then be applied to solve the inverse problem. The reduction method described in Section 4 can also be applied to this DM.

The location of sensors along the channel axis plays an important role: *the order of the DM used for inversion increases with respect to the position of sensors in downstream direction*. In fact, two DMs of the form ((5a) and (5b)) have been used:

- The first one is relative to cases where sensors abscissa is up to $x = 5D_{\text{h}}$. Only the corresponding part of the channel is used: $N_\xi = 10$ and the model order is $N = 250$.
- The second one is relative to cases where sensors abscissa is up to $x = 50D_{\text{h}} = L$. The whole heated channel is used. $N_\xi = 100$ and the model order is therefore $N = 2500$.

In contrast to DM, RM is no longer expressed in the physical base of temperatures but in a modal base (cf. Section 4), *hence its order does not necessary increase with respect to the position of sensors in downstream direction*. Nevertheless, several RMs have been built, each one corresponding to a specific case of sensor locations (cf. Section 8.3, Table 2).

8. Inversion results and analysis

8.1. Studied configuration

The following case is considered: air is entering the channel at $T_{\text{in}} = 300$ K. Fluid properties are then taken as: $\rho_{\text{f}} = 1.16\ \text{kg m}^{-3}$, $C_{pf} = 1007\ \text{J kg}^{-1}\,\text{K}^{-1}$, $\lambda_{\text{f}} = 2.63\times10^{-2}\ \text{W m}^{-1}\,\text{K}^{-1}$, $\nu = 1.59\times10^{-5}\ \text{m}^2\,\text{s}^{-1}$.

Solid properties are taken as: $\rho_{\text{s}} = 7900\ \text{kg m}^{-3}$, $C_{ps} = 477\ \text{J kg}^{-1}\,\text{K}^{-1}$, $\lambda_{\text{s}} = 14.9\ \text{W m}^{-1}\,\text{K}^{-1}$.

The channel half-height is $b = 5\times10^{-2}$ m, the channel length $L = 10$ m. The wall thickness is $e = 2\times10^{-3}$ m. The Reynolds number is $Re = 10^5$, thus corresponding to $U_{\text{m}} = 7.9\ \text{m s}^{-1}$.

8.2. Sensitivity analysis

Let us consider Eq. (13) with the definition of matrix C_{R} (Eq. (14)). One may define static and dynamic dimensionless sensitivities relative to the unknown Φ_{n} by matrices S and $C_{\text{R}} = H\exp(F\Delta\tau)G + S$ respectively.

Dynamic sensitivities are lower than static sensitivities [28]. Sensitivities relative to Φ_s can be deduced considering channel axis symmetry.

Static matrix S is conserved through the MIM: RM static sensitivities (Fig. 6) are hence equal to DM ones. RM dynamic sensitivities (Fig. 7) are not exactly equal to DM ones, but the values are however similar and the analysis is qualitatively analogous. In Figs. 6 and 7, one has, from left to right: (●): P_0 to P_5; (■): M_0 to M_5; (▲): M'_0 to M'_5; (◆): P'_0 to P'_5.

One may formulate some comments from Figs. 6 and 7 (a similar analysis may be conducted with static sensitivities):

- For a fixed ordinate $\eta = y/b$ in the fluid, sensitivities increase with the abscissa x/D_h. In fact, a point in the flow is not affected by the part of wall heat flux density applied downstream to that point. Hence, the farther from the inlet the sensor is, the more thermal information it gets.
- For a fixed abscissa x/D_h, sensitivities increase when the distance from the wall subjected to the boundary condition decreases (Φ_n in the considered case). Sensitivities associated with sensors located near the opposite wall are of course weak. By symmetry, they are high relatively to the other boundary condition Φ_s. As a consequence, employing two sensors (or groups of sensors), each one close to a particular wall, will provide a rather decoupled estimation.

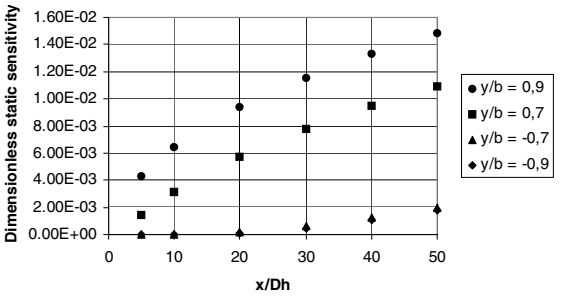

Fig. 6. Static sensitivities relative to Φ_n.

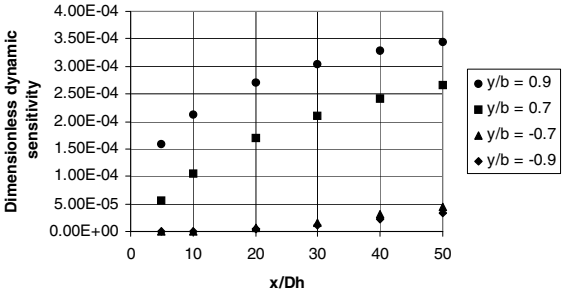

Fig. 7. Dynamic sensitivities relative to Φ_n.

- When the inversion is carried out using two sensors, the condition number of matrix $C_R^T C_R$ of Eq. (16) is better if sensors have the same abscissa and symmetric ordinates, as it can be seen below:
  - Let us consider points P_0 and M'_0 (same abscissa but nonsymmetric ordinates). The dynamic sensitivity matrix is written:

$$C_R = \begin{bmatrix} s_{P_0/\Phi_n} & s_{P_0/\Phi_s} \\ s_{M'_0/\Phi_n} & s_{M'_0/\Phi_s} \end{bmatrix} = \begin{bmatrix} 1.59 \times 10^{-4} & 1.39 \times 10^{-8} \\ 4.68 \times 10^{-8} & 5.64 \times 10^{-5} \end{bmatrix}$$

$$\text{so } C_R^T C_R = \begin{bmatrix} 2.53 \times 10^{-8} & 4.85 \times 10^{-12} \\ 4.85 \times 10^{-12} & 3.18 \times 10^{-9} \end{bmatrix}$$

$C_R^T C_R$ condition number is therefore equal to 7.95. This condition number is defined as $\frac{\max_i |\mu_i(C_R^T C_R)|}{\min_i |\mu_i(C_R^T C_R)|}$ where the $\mu_i(C_R^T C_R)$ are the eigenvalues of matrix $C_R^T C_R$.

  - Let us now consider points P_0 and P'_5 (symmetric ordinates but different abscissas). The dynamic sensitivity matrix is written:

$$C_R = \begin{bmatrix} s_{P_0/\Phi_n} & s_{P_0/\Phi_s} \\ s_{P'_5/\Phi_n} & s_{P'_5/\Phi_s} \end{bmatrix} = \begin{bmatrix} 1.59 \times 10^{-4} & 1.39 \times 10^{-8} \\ 3.32 \times 10^{-5} & 3.45 \times 10^{-4} \end{bmatrix}$$

$$\text{so } C_R^T C_R = \begin{bmatrix} 2.64 \times 10^{-8} & 1.15 \times 10^{-8} \\ 1.15 \times 10^{-8} & 1.19 \times 10^{-7} \end{bmatrix}$$

$C_R^T C_R$ condition number is now equal to 4.82.

  - Finally, lets us take P_0 and P'_0 (same abscissa and symmetric ordinates). The dynamic sensitivity matrix is written:

$$C_R = \begin{bmatrix} s_{P_0/\Phi_n} & s_{P_0/\Phi_s} \\ s_{P'_0/\Phi_n} & s_{P'_0/\Phi_s} \end{bmatrix} = \begin{bmatrix} 1.59 \times 10^{-4} & 1.39 \times 10^{-8} \\ 1.39 \times 10^{-8} & 1.59 \times 10^{-4} \end{bmatrix}$$

$$\text{so } C_R^T C_R = \begin{bmatrix} 2.53 \times 10^{-8} & 4.42 \times 10^{-12} \\ 4.42 \times 10^{-12} & 2.53 \times 10^{-8} \end{bmatrix}$$

$C_R^T C_R$ condition number is now very close to 1 (1.0004), which is the best one.

When moving down to the channel inlet, the third remark has less significance because sensitivity of each point relative to the boundary condition applied on opposite wall increases. However, condition numbers remain low (from 1.5 to 2 in $x = 50D_h$, cf. Section 8.3, Table 2), and as sensitivities are higher, the estimation quality is improved.

8.3. Estimation results and comments

First, let us introduce the dimensionless mean quadratic error on estimated inputs σ_W between $W^{\text{exact}}(\tau)$ and $\widehat{W}(\tau)$, where W^{exact} is the exact input vector and $\widehat{W}$ is the vector of the estimated inputs obtained by inversion with DM or RM. The lower σ_W is, the better the inversion is.

$$\sigma_W = \left[\frac{1}{2(\text{nt} - \text{nf} + 1)} \sum_{i=1}^{2} \sum_{j=0}^{\text{nt}-\text{nf}} \left(\widehat{W}_i(\tau_j) - W_i^{\text{exact}}(\tau_j) \right)^2 \right]^{1/2} \tag{32}$$

where nt is the number of time steps.

In the same way, the dimensionless mean quadratic error on temperatures σ_Y between $Y^{\text{meas}}(\tau)$ and $\widehat{Y}(\tau)$, where Y^{meas} is the vector of temperature measurements and $\widehat{Y}$ is the vector of the temperatures calculated with the identified inputs, can be written as:

$$\sigma_Y = \left[\frac{1}{q(\text{nt} - \text{nf} + 1)} \sum_{i=1}^{q} \sum_{j=0}^{\text{nt}-\text{nf}} \left(\widehat{Y}_i(\tau_j) - Y_i^{\text{meas}}(\tau_j) \right)^2 \right]^{1/2} \tag{33}$$

Note that because of the ill-posed nature of inverse problems, σ_Y can be very small even with very bad identification results, i.e. with a very large σ_W. That is why regularization techniques have to be employed, in order to stabilize the solutions. In real cases, σ_W is of course unknown since W is really unknown, so only σ_Y is available in practical applications.

The inverse problem resolution using exact data ($\sigma^* = 0$ K) gives very good results without any regularization (nf = 0) and whatever the sensors number and their positions and whatever the model, DM or RM. Figs. 8 and 9 show discrepancies between exact heat flux densities Φ_n and Φ_s and estimations obtained respectively with DM (order $N = 250$) and RM (order $n = 12$), from data at M_0 and M_0', corresponding to the most difficult case (see sensitivities on Figs. 6 and 7). Fig. 10 shows estimations obtained with RM. As RM does not contain all the spectral information of DM, estimations using RM are less accurate than those coming from DM when using exact data. Dimensionless mean quadratic errors are respectively $\sigma_Y = 2.11 \times 10^{-17}$ and $\sigma_W = 7.19 \times 10^{-6}$ for DM and $\sigma_Y = 8.44 \times 10^{-16}$ and $\sigma_W = 0.731$ for RM.

Inversion results using noised data ($\sigma^* = 3.88 \times 10^{-2}$ K i.e. $\sigma = \sigma^*/T_{\text{ref}} = 3.88 \times 10^{-3}$ using $\Delta T_{\text{ref}} = 10$ K according to Section 7.1) are summarized in Table 2.

The most difficult case using two sensors at M_0 and M_0' is presented in Figs. 11 (DM, order 250) and 12

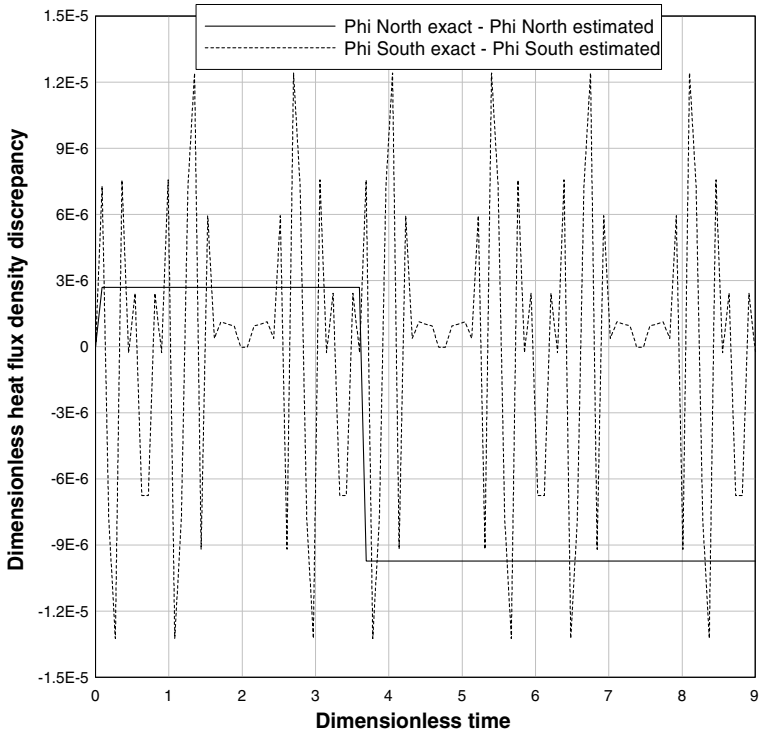

Fig. 8. Inversion using two sensors at M_0 and M_0' ("exact" data) and DM (order 250) with nf = 0. Discrepancies between exact heat flux densities and estimated ones.

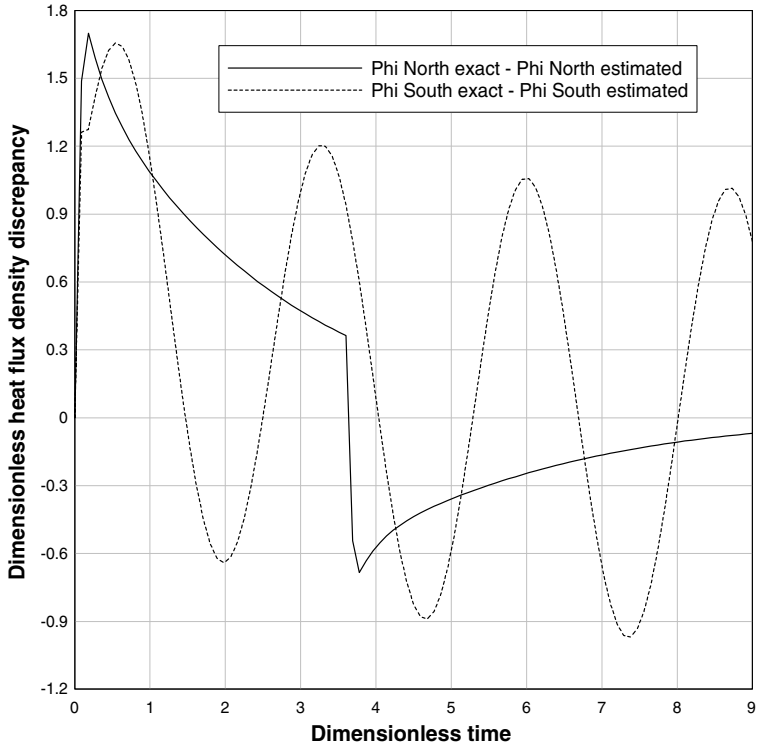

Fig. 9. Inversion using two sensors at M_0 and M'_0 (“exact” data) and RM (order 12) with nf $= 0$. Discrepancies between exact heat flux densities and estimated ones.

(RM, order 12): four FTS are required (i.e. nf $= 4$) and estimations still exhibit large oscillations.

Estimations obtained using 10 sensors at M_1 to M_5 and M'_1 to M'_5 are shown in Figs. 13 (DM, order 2500) and 14 (RM, order 8): the inverse problem is over-determined and better estimations are obtained using only nf $= 2$.

The function specification method (cf. Section 6), taking into account “Future Time Steps”, has been employed. The number nf of FTS used has been determined to satisfy the discrepancy principle, stipulating that σ_Y should be close to the standard deviation σ [4,36]. nf has been incremented from zero to the first value giving $\sigma_Y \approx \sigma$ and $\sigma_Y \geqslant \sigma$. In the studied cases, if the next value of nf is used, σ_Y increases and is no more close to σ. Of course, the procedure to determine nf is much faster and easier with RM than with DM.

Remark. Although the inverse problem is solved sequentially in time, the standard deviation of measurement errors σ is a whole time domain information. Therefore, the value of nf can only be determined by comparing global quantities σ_Y and σ, as in [27,36] for example. RMs allow to perform very fastly the nf + 1 (0 to nf) resolutions leading to the determination of nf.

Results from Table 2 can be analysed:

- Future Time Steps

  If no FTS are required with exact data, several FTS are needed when noise is added.
- Comparison between DM and RM

  For a given data set, solving the inverse problem with RM requires as many FTS as with DM. Estimations obtained with both models are very close, slightly better with DM (cf. σ_W values). σ_Y values are quasi-identical. These remarks attest *the robustness of the inversion employing RM*. It is important to note that instabilities are not due to RM. The same instabilities are obtained with DM. This is classically observed when using sequential methods instead of whole time domain methods. The latter generate less instabilities but require more CPU time and memory size and hence are not well adapted for control command. Moreover, the use of RM allows a *drastic reduction of computing time*. As an example, for the case of 10 sensors M_1 to M_5 and M'_1 to M'_5, *computing time is 0.07 s CPU using an RM of order 8 and 457 s CPU using the DM of order 2500*, *resulting in a reduction factor 6500*. This factor goes up to 11,000 for other cases.

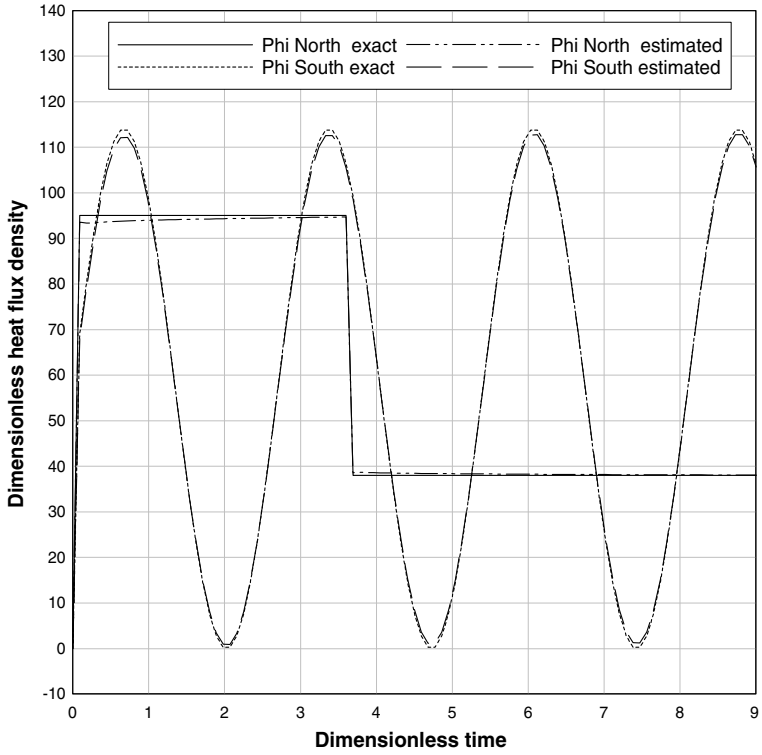

Fig. 10. Inversion using two sensors at M_0 and M_0' ("exact" data) and RM (order 12) with nf = 0.

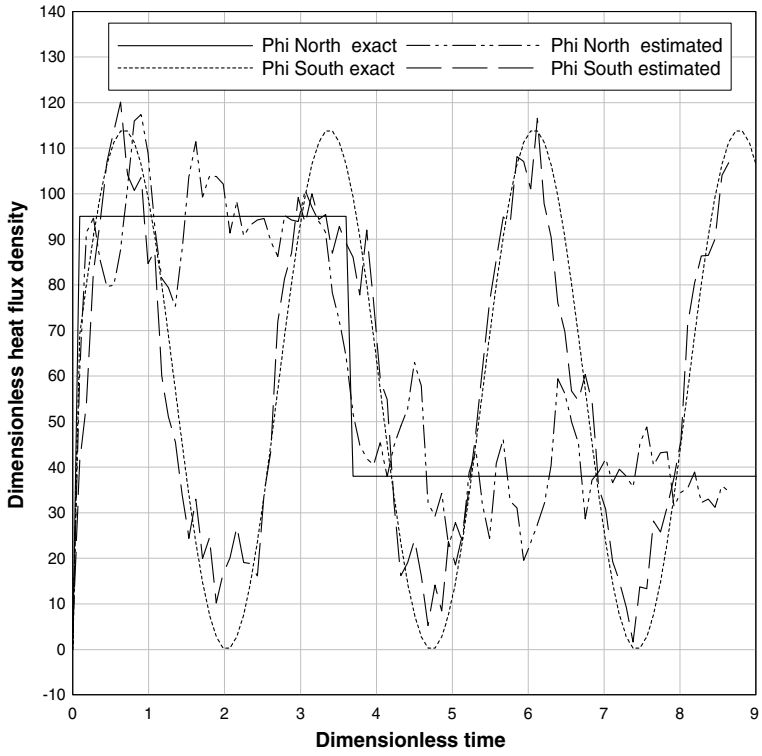

Fig. 11. Inversion using two sensors at M_0 and M_0' and DM (order 250) with nf = 4.

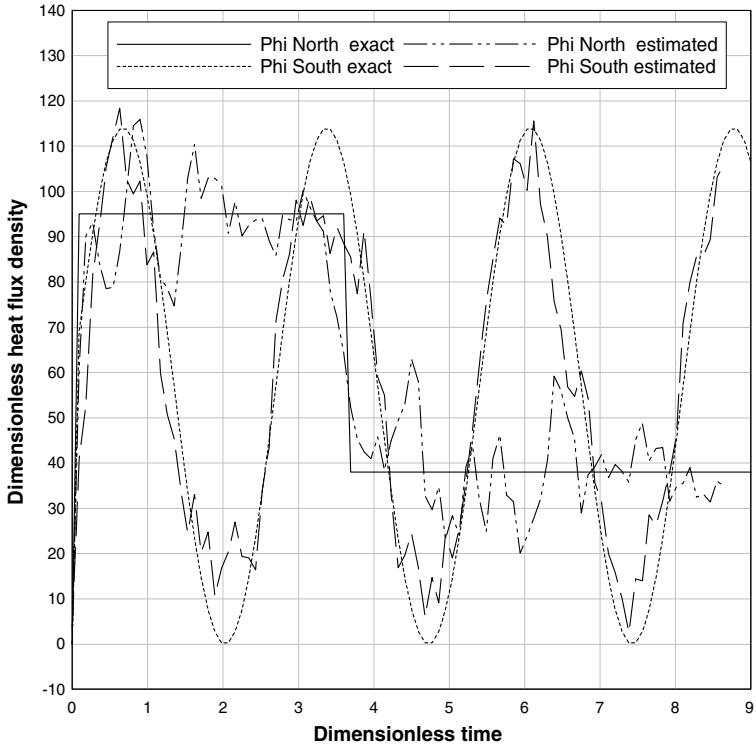

Fig. 12. Inversion using two sensors at M_0 and M_0' and RM (order 12) with nf = 4.

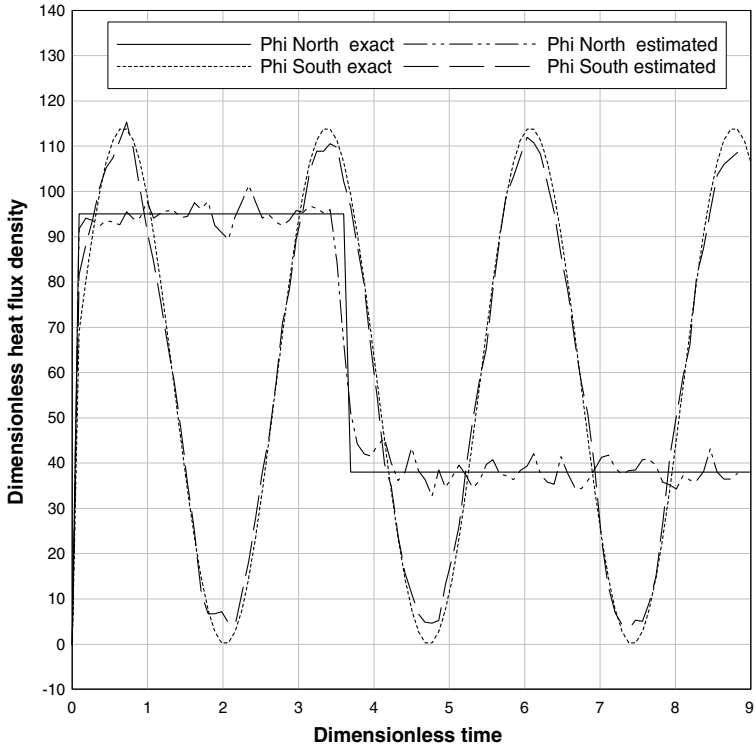

Fig. 13. Inversion using 10 sensors at M_1 to M_5 and M_1' to M_5', and DM (order 2500) with nf = 2.

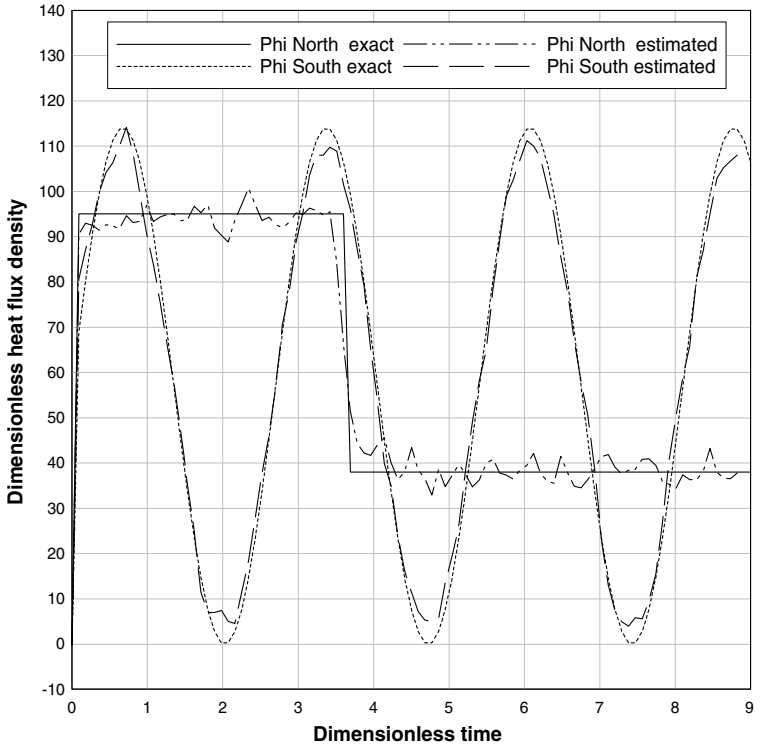

Fig. 14. Inversion using 10 sensors at M_1 to M_5 and M'_1 to M'_5, and RM (order 8) with nf = 2.

- Effect of sensor positions along the channel axis

For temperature data collected at a given depth in the fluid, estimations obtained with two sensors at abscissa $x = 5D_h$ are less accurate than those obtained with two sensors at abscissa $x = 50D_h$. In the first case, sensitivities are weak (cf. Figs. 6 and 7) and the signal/noise ratio is small (cf. Figs. 4 and 5). In the second case, sensitivities are higher (cf. Figs. 6 and 7) and the signal/noise ratio is larger considering the same additive noise (cf. Figs. 4 and 5). As previously mentioned, one of the RM advantages is that the order of the model used for inversion is not linked to sensor axial positions.

- Effect of sensor positions along the transverse direction

For temperature data collected at given axial positions, estimations obtained with sensors located in $y = \pm 0.9b$ are better than those obtained with sensors positioned in $y = \pm 0.7b$. This is in agreement with sensitivity analysis (cf. Figs. 6 and 7). Moreover, the farther from walls the sensors are, the more FTS have to be used in order to increase sensitivities.

- Effect of the number of sensors

For data collected at a given depth in the fluid, the estimation quality is of course improved by using 10 sensors instead of 2: the inverse problem is overdetermined.

- Condition number of matrix $C'^{\mathrm{T}} \cdot C'$

For each inversion case, condition numbers respectively relative to DM and RM are almost identical. This tends to prove RM robustness. Furthermore, condition numbers are close to 1, hence no regularization is needed.

9. Conclusions and prospects

In this paper, an inversion method using Reduced Models has been presented. The proposed approach can be applied to linear thermal systems. An example of transient turbulent forced convection inside a parallel-plate duct has been investigated. The objective was to simultaneously estimate two time varying wall heat flux densities.

The direct problem is formulated in the state space representation, expressing the linear relationship between unknown inputs and temperature readings taken inside the fluid. The inverse problem may then be solved sequentially by a simple linear least squares method. There is no need of using an iterative method such as conjugate gradient or Levenberg–Marquardt method. No initial guess is needed. Moreover, according to the linearity of the governing equation, the Modal Identification Method is applied to build a low order model or

Reduced Model (RM), whose behaviour is very close to the original Detailed Model (DM) of the system.

It has been underlined that contrasting with DM, RM is not expressed in the physical base of temperatures but in a modal base. As a consequence, the order of the RM used for inversion is independent of sensor axial positions, which is not the case with DM in the presented example where axial diffusion is neglected. One should note that the advantage provided by RM is more obvious if axial diffusion is taken into account, since DM order is in that case always equal to $N = 2500$ (N being the number of DM discretization nodes), whatever the sensor positions.

It has also been shown that as opposed to DM, no inversion of a dimension N matrix was needed to obtain the inverse problem solution with RM.

With such a RM, inversion computing time is drastically reduced (with a reduction factor up to 11,000 in this study) as well as model size, without significant loss of accuracy. Such procedure could be then well adapted to control command processes. It should be underlined that a RM identification requires no more than a few dozens of seconds of CPU time, and once the RM is obtained, it can be used to perform as many inversions as necessary, whatever the functional form of the signal to estimate. Moreover, although several RMs have been built according to selected sensors, it is possible to build a single RM relative to the set of 20 sensors, and to use it for each inversion case, with very limited loss of accuracy.

Future developments include the identification of space and time varying boundary conditions, which occur when heat fluxes are nonuniform along the channel length. The present methods (reduction and inversion) can be applied to other duct shapes and to 3D problems, whatever the geometry, as far as they are linear. The method may then be used to analyse inverse heat convection in a circular duct asymmetrically heated, but can also be applied to irregularly shaped channels.

In particular, it is possible to identify RMs from simulations made with commercial modelling softwares that are closed for users. In that case, the inverse problem can be solved using RM while it can be very difficult, or impossible, to perform the inversion using the commercial software.

Moreover, the Modal Identification Method can be applied to real data instead of DMs simulations, allowing to perform experimental modelling [29]. The knowledge of a DM is therefore no longer required.

Finally, an extension of the approach to nonlinear systems is under development.

References

[1] A. Moutsoglou, An inverse convection problem, J. Heat Transfer 111 (1989) 37–43.

[2] J.V. Beck, B. Blackwell, C.R. St. Clair, Inverse Heat Conduction: Ill-Posed Problems, Wiley-Interscience Publication, New York, 1985, pp. 108–160.

[3] Y. Jarny, M.N. Ozisik, J.P. Bardon, A general optimization method using adjoint equation for solving multidimensional inverse heat conduction, Int. J. Heat Mass Transfer 34 (11) (1991) 2911–2919.

[4] O.M. Alifanov, Inverse Heat Transfer Problems, Springer-Verlag, New York, 1994.

[5] M. Prud'homme, T.H. Nguyen, Whole time-domain approach to the inverse natural convection problem, Numer. Heat Transfer Part A 32 (1997) 169–186.

[6] H.M. Park, O.Y. Chung, Inverse natural convection problem of estimating wall heat flux, Chem. Eng. Sci. 55 (2000) 2131–2141.

[7] H.M. Park, O.Y. Chung, Inverse natural convection problem of estimating wall heat flux using a moving sensor, J. Heat Transfer 121 (1999) 828–836.

[8] A.J. Newman, Model reduction via the Karhunen–Loève expansion, Part I: an exposition, Technical Research Report of the Institute for Systems Research, University of Maryland, 1996. Available from <http://techreports.isr.umd.edu/TechReports/ISR/1996/TR_96-32/TR_96-32.phtml>.

[9] H.M. Park, W.S. Jung, The Karhunen–Loève Galerkin method for the inverse natural convection problems, Int. J. Heat Mass Transfer 44 (1) (2001) 155–167.

[10] M. Prud'homme, T.H. Nguyen, Solution of inverse free convection problems by conjugate gradient method: effects of Rayleigh number, Int. J. Heat Mass Transfer 44 (11) (2001) 2011–2027.

[11] H.M. Park, J.S. Chung, A sequential method of solving inverse natural convection problems, Inverse Problems 18 (2002) 529–546.

[12] C.H. Huang, M.N. Özisik, Inverse problem of determining unknown wall heat flux in laminar flow through a parallel plate duct, Numer. Heat Transfer Part A 21 (1992) 55–70.

[13] J.C. Bokar, M.N. Özisik, An inverse analysis for estimating the time-varying inlet temperature in laminar flow inside a parallel plate duct, Int. J. Heat Mass Transfer 38 (1) (1995) 39–45.

[14] F.B. Liu, M.N. Özisik, Estimation of inlet temperature profile in laminar duct flow, Inverse Problems Eng. 3 (1996) 131–143.

[15] H.A. Machado, H.R.B. Orlande, Inverse analysis for estimating the timewise and spacewise variation of the wall heat flux in a parallel plate channel, Int. J. Numer. Methods Heat Fluid Flow 7 (7) (1997) 696–710.

[16] H.A. Machado, H.R.B. Orlande, Inverse problem for estimating the heat flux to a non-Newtonian fluid in a parallel plate channel, J. Brazilian Soc. Mech. Sci. 20 (1) (1998) 51–61.

[17] F.B. Liu, M.N. Özisik, Inverse analysis of transient turbulent forced convection inside parallel-plate ducts, Int. J. Heat Mass Transfer 39 (12) (1996) 2615–2618.

[18] M.J. Colaço, H.R.B. Orlande, Inverse forced convection problem of simultaneous estimation of two bounary heat fluxes in irregularly shaped channels, Numer. Heat Transfer Part A 39 (2001) 737–760.

[19] C.H. Huang, W.C. Chen, A three-dimensional inverse forced convection problem in estimating surface heat flux

by conjugate gradient method, Int. J. Heat Mass Transfer 43 (17) (2000) 3171–3181.
[20] J. Su, A.B. Lopes, A.J. Silva Neto, Estimation of unknown wall heat flux in turbulent circular pipe flow, Int. Commun. Heat Mass Transfer 27 (7) (2000) 945–954.
[21] P. Ben Abdallah, H. Sadat, V. Le Dez, Résolution d'un problème inverse de convection–diffusion par une méthode de perturbation singulière, Int. J. Therm. Sci. 39 (2000) 742–752.
[22] P.T. Hsu, C.K. Chen;, Y.T. Yang, A 2-D inverse method for simultaneous estimation of the inlet temperature and wall heat flux in a laminar circular duct flow, Numer. Heat Transfer Part A 34 (1998) 731–745.
[23] I. Gejadze I, Y. Jarny, A method of temperature restoration in polymer melt flow through narrow channel, in: D. Petit, D.B. Ingham, Y. Jarny, F. Plourde (Eds.), Proceedings of the Eurotherm Seminar No. 68: Inverse Problems and Experimental Design in Thermal and Mechanical Engineering, Poitiers, France, March 5–7, 2001, pp. 247–254.
[24] A.N. Tikhonov, V.Y. Arsenin, Solutions of Ill-Posed Problems, V.H. Winston & Sons, Washington, DC, 1977.
[25] H.M. Park, J.H. Lee, A method of solving inverse convection problems by means of mode reduction, Chem. Eng. Sci. 53 (9) (1998) 1731–1744.
[26] D. Petit, R. Hachette, D. Veyret, A modal identification method to reduce a high order model: application to heat conduction modelling, Int. J. Modell. Simul. 17 (3) (1997) 242–250.
[27] E. Videcoq, D. Petit, Model reduction for the resolution of multidimensional inverse heat conduction problems, Int. J. Heat Mass Transfer 44 (10) (2001) 1899–1911.
[28] E. Videcoq, Problèmes inverses en diffusion thermique instationnaire: résolution par représentation d'état et apport de la réduction de modèle, Ph.D. Thesis, Université de Poitiers, France, 1999.
[29] E. Videcoq, D. Petit, A. Piteau, Experimental modelling and estimation of time varying thermal sources, Int. J. Therm. Sci. 42 (3) (2003) 255–265.
[30] M. Girault, Résolution de problèmes inverses en thermique par modèles réduits: applications en conduction non-linéaire et en convection forcée, Ph.D. Thesis, Université de Poitiers, France, 2003.
[31] M. Girault, D. Petit, E. Videcoq, The use of model reduction and function decomposition for identifying boundary conditions of a linear thermal system, Inverse Problems Eng. 11 (5) (2003) 425–455.
[32] S. Kakac, W. Li;, R.M. Cotta, Unsteady laminar forced convection in ducts with periodic variation of inlet temperature, J. Heat Transfer 112 (1990) 913–920.
[33] S. Kakac, W. Li, Unsteady turbulent forced convection in a parallel-plate channel with timewise variation of inlet temperature, Int. J. Heat Mass Transfer 37 (Suppl. 1) (1994) 447–456.
[34] W.S. Kim, M.N. Özisik, Turbulent forced convection inside a parallel-plate channel with periodic variation of inlet temperature, J. Heat Transfer 111 (1989) 882–888.
[35] M. Jischa, H.B. Rieke, About the prediction of turbulent Prandtl and Schmidt numbers from modeled transport equations, Int. J. Heat Mass Transfer 22 (11) (1979) 1547–1555.
[36] J.V. Beck, B. Blackwell, A. Haji-Sheikh, Comparison of some inverse heat conduction methods using experimental data, Int. J. Heat Mass Transfer 39 (17) (1996) 3649–3657.